Novel Functional Polymers: Poly(dimethylsiloxane)−Polyamide Multiblock Copolymer. 8.[1] Surface Studies of Aramid−Silicone Resin by Means of XPS, Static SIMS, and TEM

Kazuhisa Senshu,[†] Tsutomu Furuzono,[‡] Naoto Koshizaki,[§] Shuzo Yamashita,[†] Takeo Matsumoto,[∥] Akio Kishida,[‡] and Mitsuru Akashi*,[‡]

R&D Center, Terumo Corporation, 1500 Inokuchi, Nakai-machi, Ashigarakami-gun, Kanagawa 259-01, Japan, Department of Applied Chemistry and Chemical Engineering, Faculty of Engineering, Kagoshima University, 1-21-40 Korimoto, Kagoshima 890, Japan, Department of Composite Materials, National Institute of Materials and Chemical Research, 1-1 Higashi, Tsukuba, Ibaraki 305, Japan, and Tsukuba Research Laboratory, NOF Corporation, 5-10 Tokodai, Tsukuba, Ibaraki 300-26, Japan

Received November 4, 1996; Revised Manuscript Received February 17, 1997[⊗]

ABSTRACT: The surface structures of solvent-cast films with aramid−poly(dimethylsiloxane) (poly(dimethylsiloxane) = PDMS) multiblock copolymers (PASs) that contained 8, 14, 24, 41, and 71 wt % of PDMS were characterized by angular-dependent X-ray photoelectron spectroscopic (XPS) measurements, static secondary ion mass spectrometric (SSIMS) measurements, and transmission electron microscopic (TEM) observations. The results of angular-dependent XPS measurement elucidated that the surface concentration of the PDMS segments was much higher than that in bulk and further increased with a decrease in the sampling depth. In particular, the Si/C ratios that were determined by XPS at a 10° takeoff angle in PAS films that contained more than 24 wt % PDMS were almost the same as that in the PDMS homopolymer. From the results of SSIMS measurement, the outermost surfaces of all of the PAS films were found to be completely covered with a PDMS segment even if the PDMS content was only 8 wt % in bulk. In addition, we visually confirmed the surface enrichment of the PDMS segment by TEM observation. The free surfaces of all PAS films were predominantly covered with a PDMS thin layer, although the microphase-separated structures in bulk were different according to the PDMS content in PAS.

Introduction

The surface structure of multicomponent polymeric materials plays an important role in many applications such as adhesives, surfactants, composites, membranes, and biomaterials.[2] Block copolymers in particular have attracted much attention for use as a nonthrombogenic material in the medical field.[3] The surface composition of block copolymers shows a surface enrichment of one component with a lower surface energy due to the minimization of the total surface energy.[4−14] In addition, block copolymer surfaces can often relax and dynamically reconstruct in response to environmental changes.[15−21] This type of surface enrichment of one component and surface dynamics make it difficult to characterize the correlation between block copolymer surfaces and their responses in biomedical media.

Silicone rubber and silicone-containing block copolymers have been utilized as coating materials due to their repellent properties and as a biomedical implant due to their elasticity, excellent gas permeability, and inert activity in a human body. The surface structures of a series of block and graft copolymers, such as poly(dimethylsiloxane-) (PDMS-) *b*-polysulfone,[4] PDMS-*b*-poly(methylmethacrylate),[5] PDMS-*b*-polyamide-6,[6] PDMS-*b*-poly(α-methylstyrene),[7] PDMS-*b*-(bisphenol A polycarbonate),[8] PDMS-*b*-polystyrene,[9] poly(vinyl alcohol)-*g*-PDMS,[10] and segmented polyurethane-*g*-PDMS[11] were characterized by angular-dependent X-ray photoelectron spectroscopy (XPS), cross-sectional transmission electron microscopy (TEM), and attenuated total reflectance infrared spectroscopy (ATR-IR). In each case, the enrichment of PDMS segments in the surface region was detected due to the lower surface energy of the PDMS component.

Recently, multiblock copolymers of aramid−silicone resins (PAS, Figure 1) that consisted of aromatic polyamide (aramid) as a hard segment and PDMS as a soft one were synthesized by Imai *et al.*[22] We have been exploring the possible use of PAS as a biomedical polymer. We have done a lot of research in regards to characterization and functionalities of PAS by researching its mechanical properties, its thermomechanical properties, its gas permeabilities, and its blood compatibility.[23−27] Moreover, we observed the microphase-separated structure of PAS film under TEM, which was also estimated from its mechanical properties.[28] From these results, we have concluded that PAS films can be a biomedical polymer with various mechanical properties ranging from a rigid material like a polyamide to a soft one like a silicone rubber according to the PDMS content in PAS.

In this study, surface characterization of solvent-cast PAS films with different amounts of PDMS was performed in detail by means of angular-dependent XPS and static secondary ion mass spectrometry (SSIMS). An angular-dependent XPS technique probes the quantitative surface structure of the polymer surface to a depth of approximately 20−100 Å.[29] On the other hand, SSIMS gives us qualitative surface chemistry to a depth of approximately 10 Å and is far more sensitive than XPS.[30] SSIMS information is very complementary to the quantitative results that were obtained by XPS. The combination of XPS and SSIMS is a useful technique

* To whom correspondence should be addressed.
[†] Terumo Corporation.
[‡] Kagoshima University.
[§] National Institute of Materials and Chemical Research.
[∥] NOF Corporation.
[⊗] Abstract published in *Advance ACS Abstracts,* July 1, 1997.

S0024-9297(96)01621-X CCC: $14.00

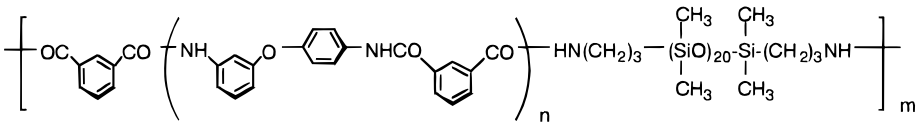

Figure 1. Chemical structure of aramid-silicone resin(PAS).

Table 1. Characterizations of PAS

polymers	PDMS content[a] (wt %)	$\bar{M}_n$ PDMS[b]	$\bar{M}_n$ aramid[a]
PAS-8	8	1680	19300
PAS-14	14	1680	10600
PAS-24	24	1680	5300
PAS-41	41	1680	2400
PAS-71	71	1680	700

[a] Calculated from the Si−CH_3/aromatic H ratio in the ^{1}H-NMR spectrum. [b] Determined by titration of terminal amino group.

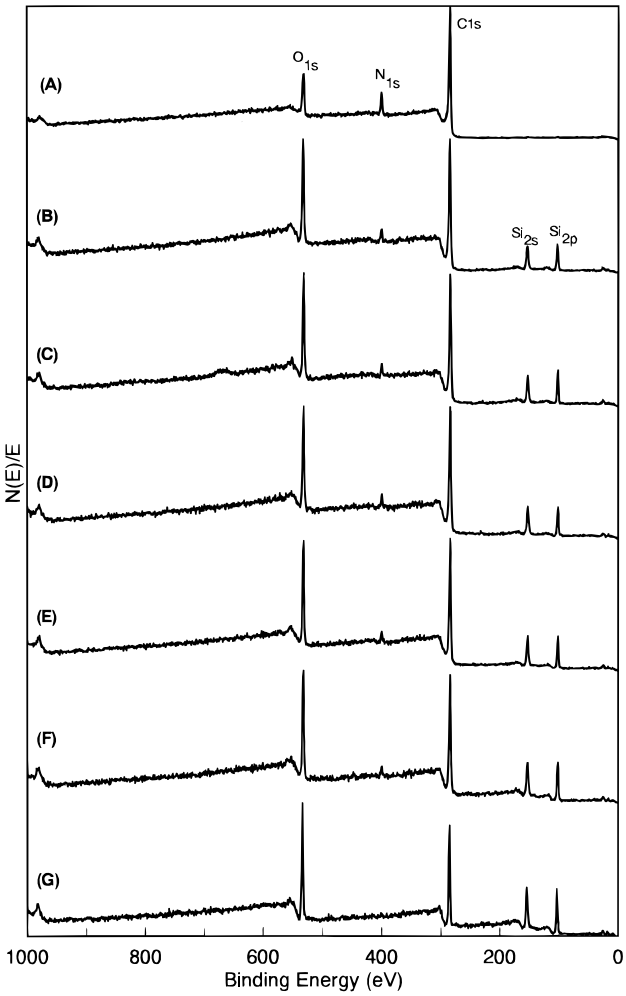

Figure 2. XPS survey spectra of solvent-cast films of aramid homopolymer (A), PAS-8 (B), PAS-14 (C), PAS-24 (D), PAS-41 (E), PAS-71 (F), and PDMS homopolymer (G), at 40° TOA.

for studying the surface segregation of block copolymers. Furthermore, the surface structure of PAS films was also visually elucidated by TEM observation and was compared with those that were obtained by XPS and SSIMS. Clarification of the surface composition, gradient, and morphology of the solvent-cast of PAS films with varied amounts of PDMS are the focus of this paper.

Experimental Section

Polymers and Film Preparation. PAS was synthesized by low-temperature solution polycondensation through a two-step procedure according to the literature.[22,23] Briefly, α,ω-dichloroformyl-terminated aramid oligomers were prepared by the reaction of isophthaloyl chloride (WAKO Pure Chemicals, Osaka, Japan) with 3,4′-diaminodiphenyl ether (Wakayama Seika Industry Co., Wakayama, Japan) in chloroform at −15 °C for 5 min in the presence of triethylamine as a hydrogen chloride acceptor under nitrogen. Next, the preformed aramid oligomers were then reacted with PDMS−diamine (number-average molecular weight of 1680, Shin-Etsu Chemical Co., Tokyo, Japan) at −15 °C for 1 h. The reactant was then isolated by pouring the reaction mixture into methanol. After the product had been washed with a large amount of methanol, a low-molecular weight fraction that had been enriched in PDMS was removed by washing the product three times with *n*-hexane, and the residue was then dried at 60 °C for 48 h *in vacuo*. The PDMS contents of PAS in bulk were calculated from $SiCH_3$/aromatic H ratio in the ^{1}H-NMR spectra measured using a JEOL EX-90 (JEOL, Tokyo, Japan). The molecular weight of PDMS as well as the aramid components of a series of PASs are summarized in Table 1. For determinaitons of total molecular weights of PASs and their distributions, gel permeation chromatographic measurement was attempt. However, we could not obtain reliable results about the molecular weight of PAS because of the poor solubility for the PDMS unit of PAS for *N*,*N*′-dimethylformamide as an eluent. The results of the mechanical properties and moldability given elsewhere,[23,24] strongly suggest that PASs possess high molecular weights.

The PAS films for XPS and SSIMS measurements and TEM observation were cast from a 10 wt % *N*,*N*′-dimethylacetamide

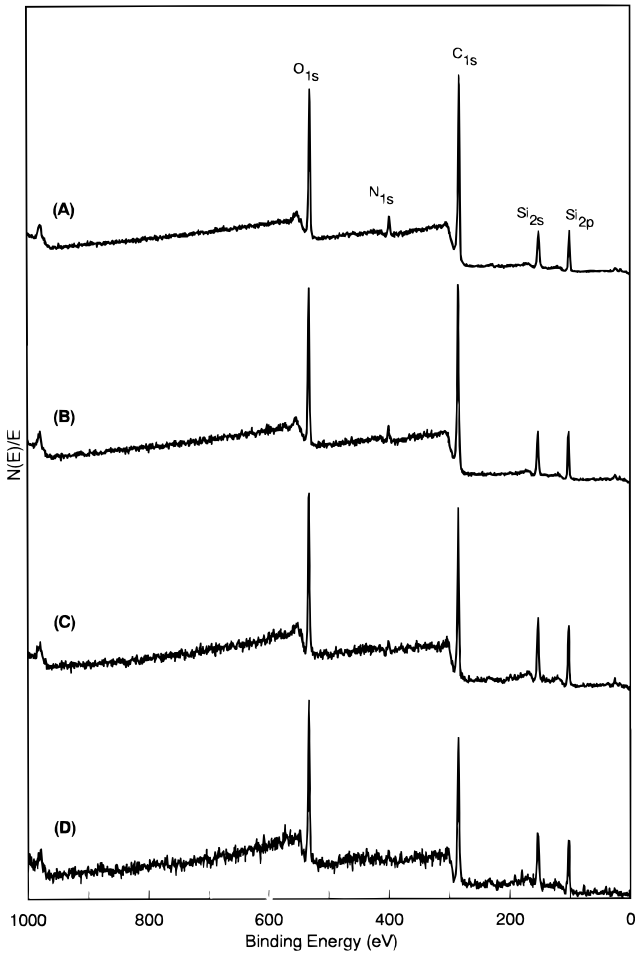

Figure 3. XPS survey spectra of solvent-cast film of PAS-41 at 75° (A), 40° (B), 20° (C), and 10° (D) TOA.

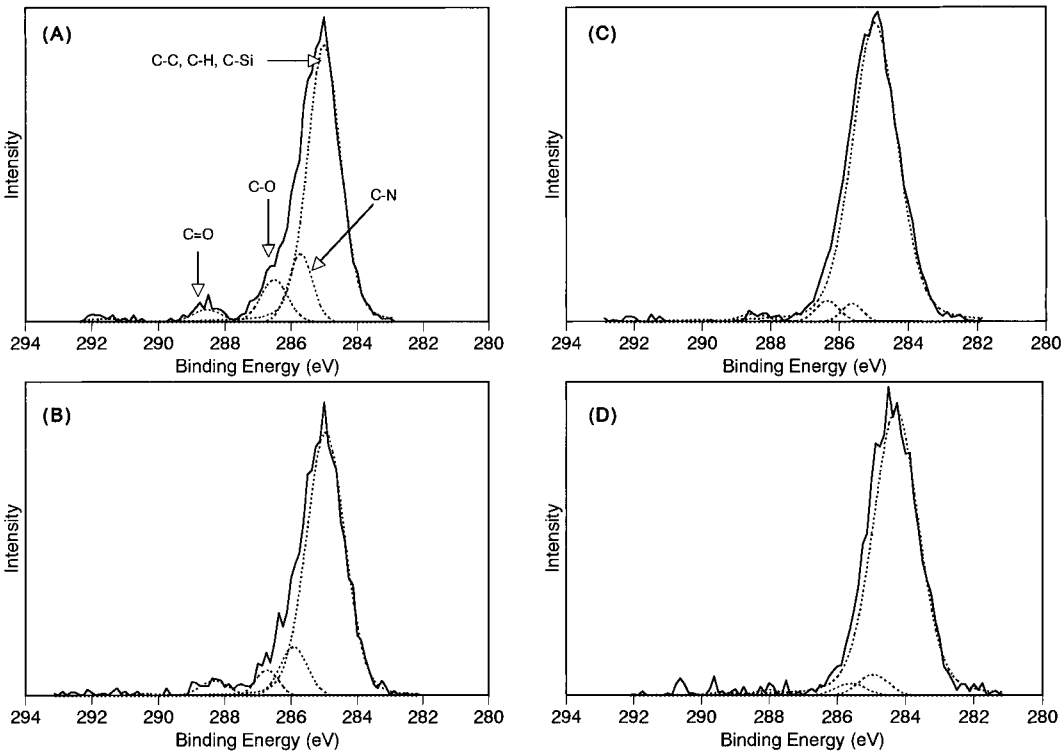

Figure 4. XPS C_{1s} spectra of solvent-cast film of PAS-41 at 75° (A), 40° (B), 20° (C), and 10° (D) TOA.

(DMAc) solution on a TEFLON sheet. The solvent was then gradually evaporated at 60 °C for 5 days. Finally, the films were dried at 60 °C for 24 h *in vacuo*, and PAS films with ca. 100 μm thickness were obtained. All of the PAS films were colorless and transparent.

XPS Analysis. The XPS spectra were acquired using a PHI 5600ci (Perkin-Elmer, MN) instrument with a hemispherical analyzer employing monochromated Al Kα (1486.7 eV) X-rays. The X-ray gun was operated at 14 kV, and the anode power was 20 W. The base pressure was maintained at lower than 10^{-9} Torr. Pass energies of 187.85 and 29.25 eV were chosen for survey spectrum acquisition (0−1000 eV) and high-resolution spectrum acquisition (O_{1s}, N_{1s}, C_{1s}, and Si_{2p}), respectively. Four takeoff angles (TOAs) at 75, 40, 20, and 10° were used, where TOA was defined as the angle between the sample plane and the axis of the analyzer. A low-energy electron flood gun (emission current, 0−20 mA; electron energy, 5−20 eV) was used in order to minimize sample charging. Quantification and curve fitting of the XPS signals were performed using the software attached to the PHI 5600ci. All of the binding energies (BEs) were referenced by setting the CH_x peak maximum in the resolved C_{1s} spectra to 285.0 eV.

SSIMS Analysis. The positive and negative spectra were also obtained by using the same apparatus for XPS, PHI 5600ci, equipped with a quadrupole mass analyzer. Xe^+ ions of 3 keV were used as a primary ion and were rastered over a 3 × 1.5 mm area with an average current density of 1 nA/cm^2. Charge neutralization was achieved with a low-energy flood gun.

TEM Observation. The PAS films were fixed and stained with RuO_4 vapor[31,32] for 15 min. The specimens were then embedded in epoxy resin (Quetol 812, Nisshin EM Ltd., Tokyo, Japan). Ultrathin sections were made by using a ultramicrotome (2088V, LKB Ltd., Sweden) with a diamond knife at room temperature and were observed under TEM (JEM 1200-EX, JEOL Ltd., Tokyo, Japan) at an accelerated voltage of 80 kV without poststaining.

Results and Discussion

XPS Analysis. In our previous study, we reported that the film surfaces of PASs with PDMS content that ranged from 25 to 75 wt % that were cast from DMAc showed much higher enrichment of the PDMS segment than in bulk by means of XPS measurement. The contact angle values used for water on PAS films gave almost the same results on silicone rubber film.[23] In addition, from the results of the *in vitro* evaluation of blood compatibility, the surface of the PAS film was found to behave like a silicone rubber surface.[23] In this paper, the surface studies of PAS films with 8 to 71 wt % of PDMS were performed by angular-dependent XPS. This gave us information of a surface composition as well as depth profiles. The higher angles penetrated deeper into the surface; *e.g.*, 75° TOA is present in the outer ∼100 Å of the sample surface. The sampling depth decreases from about 100 to 20 Å as the TOA decreases from 75 to 10°.

The XPS survey spectra of PDMS homopolymer, PAS-8, -14, -24, -41, -71 and aramid homopolymer at 40° TOA are shown in Figure 2. Only O_{1s}, N_{1s}, C_{1s}, Si_{2s}, and Si_{2p} peaks were observed in all PAS samples. On the other hand, Si_{2s} and Si_{2p} peaks and a N_{1s} peak were not detected from aramid and the PDMS homopolymer, respectively. This suggests that the samples are free from surface contamination. The XPS survey scan spectrum at other TOAs also showed the same tendency. Figure 3 shows the survey scan spectrum of PAS-41 at 75, 40, 20, and 10° TOA. The peak height of N_{1s} gradually decreased and those of O_{1s} and Si_{2p} increased with decreasing TOA, which suggested the surface enrichment of PDMS segment. This tendency was seen in all PAS films and was also confirmed by high-resolution C_{1s} XPS spectra as shown in Figure 4. At higher TOA (deep surface), the C_{1s} spectrum was resolved at 285.0, 286.0, 286.6, and 288.3 eV due to the C−C(C−H, C−Si), C−N, C−O, and C═O components. The C_{1s} spectrum at lower TOA (shallow surface), however, showed that a single peak was contributed to the C−C(C−H, C−Si) component.

The quantitative analysis was carried out based on the Si/C atomic ratios that were obtained by high-resolution spectra. Figure 5 shows Si/C atomic ratios for PAS films and PDMS homopolymers as a function of TOA (sin θ). In the aramid homopolymer, the N/C

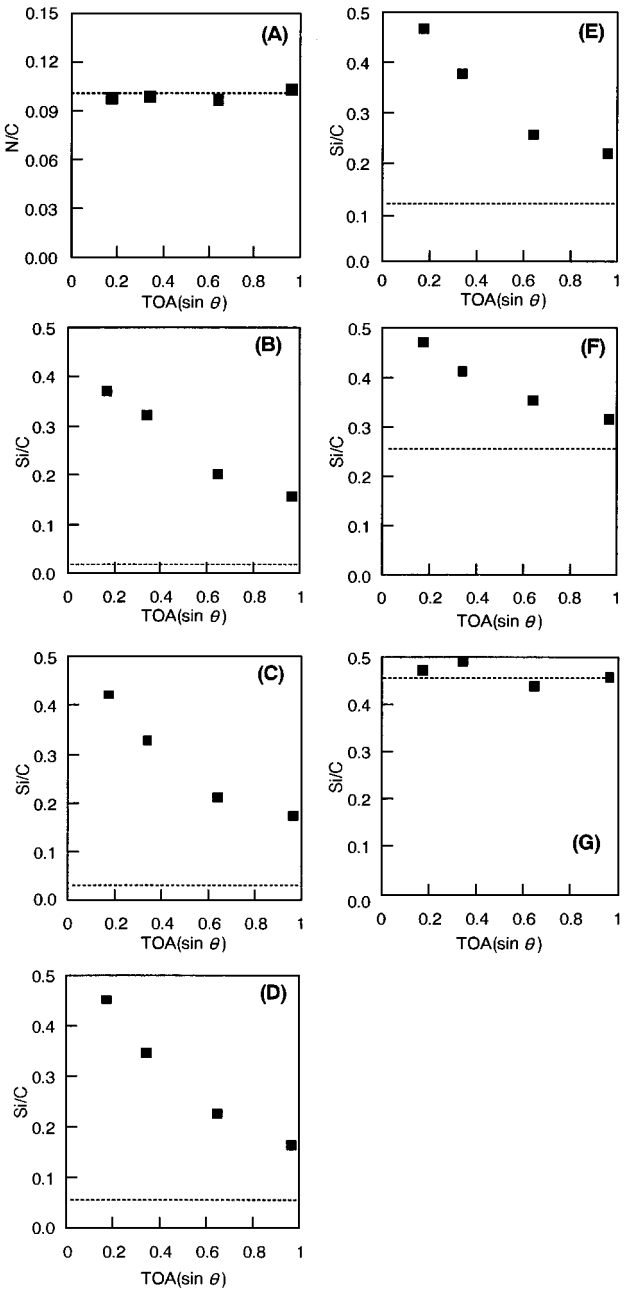

Figure 5. N/C atomic ratio of solvent-cast film aramid homopolymer (A) and Si/C atomic ratios of those of PAS-8 (B), PAS-14 (C), PAS-24 (D), PAS-41 (E), PAS-71 (F), and PDMS homopolymer (G) as a function of TOA (sin θ). All of values were determined by high-resolution XPS spectra. Dashed lines indicate the calculated values from the bulk composition determined by ^{1}H-NMR.

atomic ratio is plotted because of the absence of Si element in bulk. Both aramid and PDMS homopolymers showed almost the same atomic ratios in all sampling depths as those of in bulk determined by ^{1}H-NMR, which suggests that there was no surface gradient. However, PAS films showed surface enrichment of the PDMS segment as compared with those in bulk. It increased remarkably with a decrease in the sampling depth. The Si/C atomic ratio at 10° TOA as a function of PDMS content is shown in Figure 6. When the PDMS content in bulk was increased, a noticeable increase of the Si/C ratios was observed and finally reached a plateau when the bulk PDMS concentration was greater than 24 wt %. These results indicate the segregation of the PDMS segments at the surface of PAS films. As described in the Introduction, block and graft copolymers that contain PDMS segments show surface enrichment of PDMS segments. This is attributable to the lower surface energy of the PDMS segment. Without exception, our PAS films also showed a similar phenomenon in regards to the surface enrichment of PDMS segments. However, it is difficult to conclude from these results whether aramid segments are still present at the surface of the PAS films in the plateau.

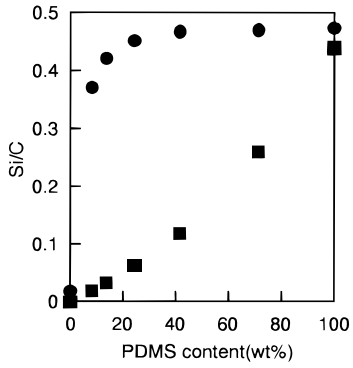

Figure 6. Si/C atomic ratios of solvent-cast films of PASs as a function of PDMS content: (●) value determined by XPS at 10° TOA; (■) calculated value from the bulk composition determined by ^{1}H-NMR.

SSIMS Analysis. For each sample, positive and negative spectra were obtained. Positive and negative SSIMS spectra for aramid and PDMS homopolymers are shown in Figure 7. The assignments of the characteristic peaks of positive SSIMS are given in Table 2, which referred to a handbook by Newman *et al.*[33] The positive spectrum of aramid homopolymer shows a large number of hydrocarbon peaks coming mainly from the benzene rings. In particular, the presence of the phenyl amide group was detected by the peaks at *m/z* 104 and 105. The positive spectrum of PDMS homopolymer shows several silyl peaks. The trimethylsilyl group at *m/z* 73 is particularly remarkable. On the other hand, the negative spectrum of aramid homopolymer shows peaks at *m/z* 13, 16, 25, 43, and 133 corresponding to CH^-, O^-, C_2H^-, CH_3CO^-, and $CONH_2C_6H_4CH^-$, respectively, and that of PDMS gives peaks at *m/z* 13, 16, 25, and 28 assigned to CH^-, O^-, C_2H^-, and Si^-. The discrimination between the two homopolymers can be easily accomplished by paying attention to each characteristic peak in the positive spectra.

Figure 8 shows the positive SIMS spectra of the PAS films containing from 8 to 71 wt % of PDMS. Surprisingly, all PAS film spectra only gave characteristic peaks that corresponded to the PDMS segment. The peaks due to the aramid segment, however, were never detected. The negative spectra of PAS films also showed the same results. These results indicate that the film surfaces of PASs are completely covered with PDMS segments even if the PDMS content in bulk is only 8 wt %. As observed by XPS analysis, the surface composition up to a depth of ~20 Å in the PAS films that contained greater than 24 wt % PDMS was extremely similar to that of PDMS homopolymer. In addition, the surface enrichment of PDMS segments decreased when the PDMS content in bulk was less than 14 wt %. The differences between the XPS and SSIMS results may be due to the sampling depth. XPS at 10° TOA detects a depth of ca. 20 Å, while the sampling depth of SSIMS is approximately 10 Å. It might be difficult to discover an ultrathin PDMS layer within 10 Å thickness at the outermost surfaces of PAS-8 and -14 films by using XPS. In this way, we have elucidated that the top surfaces of PAS-8 and -14 films were also predominantly covered with a PDMS thin layer from the result of SSIMS measurement.

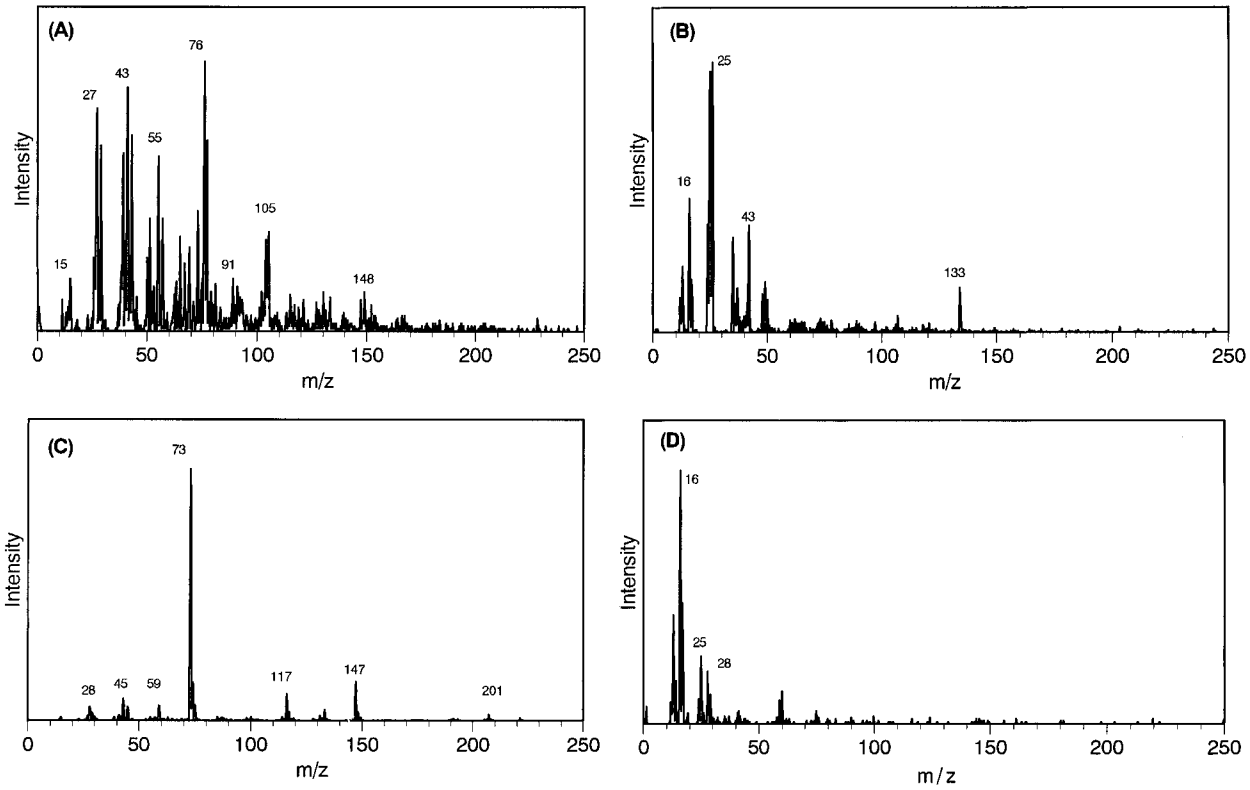

Figure 7. Positive (A) and negative (B) SSIMS spectra of solvent-cast film of aramid homopolymer. Positive (C) and negative (D) SSIMS spectra of solvent-cast film of PDMS homopolymer.

Table 2. Chemical Structures of Some of the Characteristic Positive SIMS Peaks for Aramid and PDMS Homopolymers

Aramid homopolymer		PDMS homopolymer	
m/z	Structure	m/z	Structure
15	CH_3^+	28	Si^+
27	$CH_2{=}CH^+$	43	$CH_2{=}SiH^+$
41	$CH_2{=}CH-CH_2^+$	45	$HSi\equiv O^+$
43	$^+CH{=}CH-OH$ or $CH_3-C\equiv O^+$	59	$CH_3-Si\equiv O^+$
55	$CH_2{=}CH-C\equiv O^+$	73	$(CH_3)_3Si^+$
57		117	$(CH_3)_3Si-O-SiH(CH_2)$
76		133	$HSi(CH_3)_2-O-Si^+(CH_3)_2$
77		147	$(CH_3)_3Si-O-Si^+(CH_3)_2$
91		207	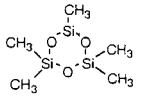
104	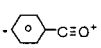	221	$(CH_3)_3Si-O-Si(CH_3)_2-O-Si^+(CH_3)_2$
105			
115			
148	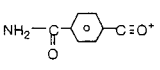		

TEM Observation. From the results of angular-dependent XPS and SSIMS, all PAS films with a PDMS content of 8−71 wt % showed significant surface enrichment of PDMS segments. The outermost ∼10 Å, in particular, appeared to be 100% PDMS even if the bulk concentration was 8 wt %. In this section, we will discuss the surface and bulk morphology of PAS films that were observed under TEM. TEM is a useful tool

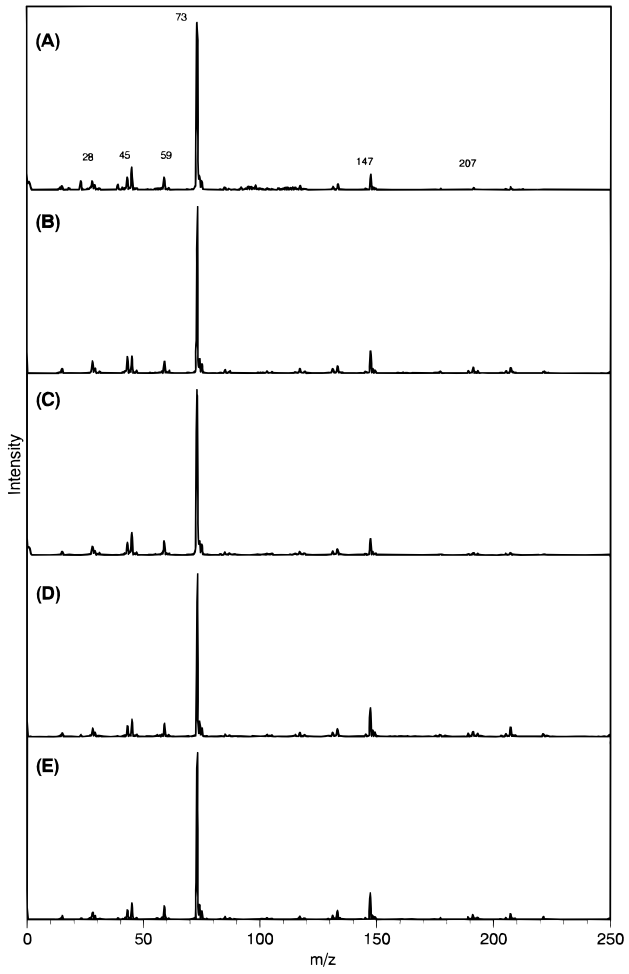

Figure 8. Positive SSIMS spectra of solvent-cast films of PAS-8 (A), PAS-14 (B), PAS-24 (C), PAS-41 (D), and PAS-71 (E).

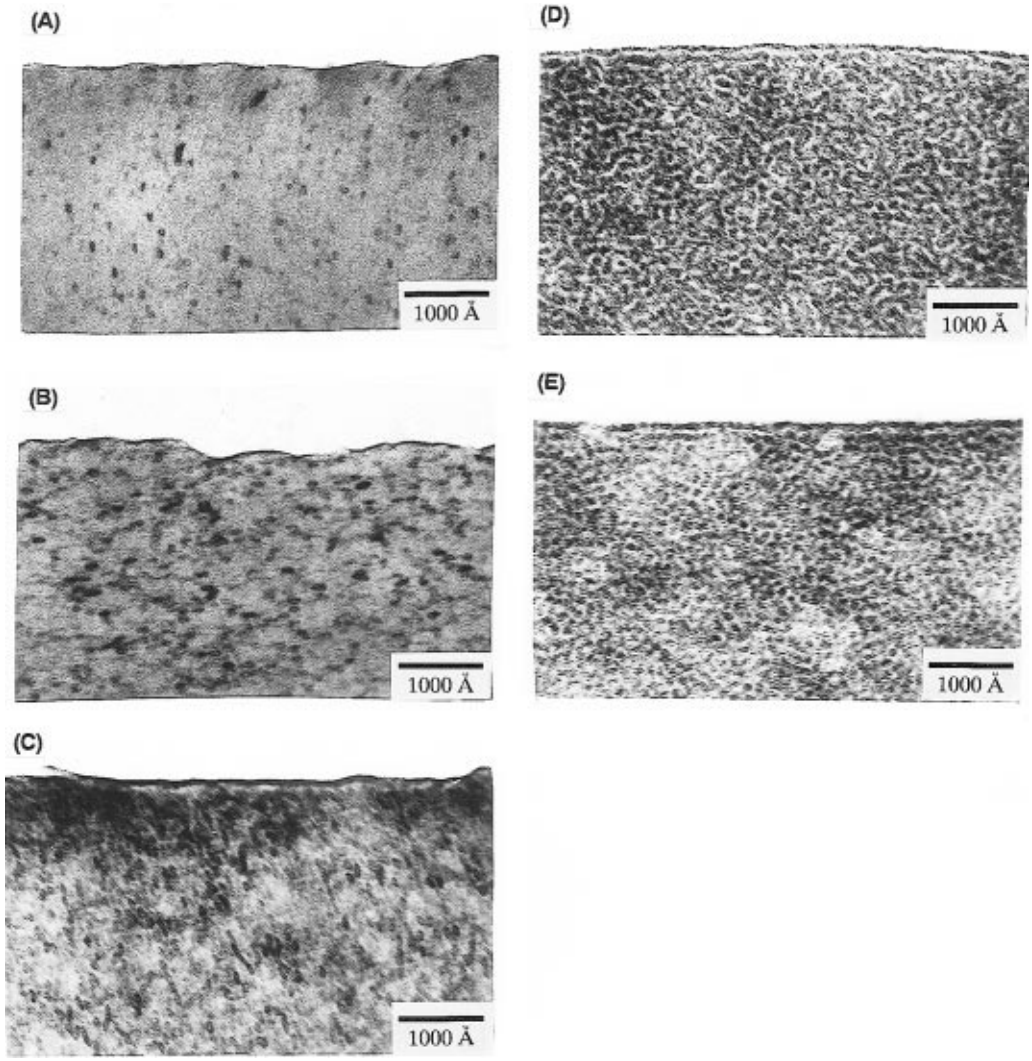

Figure 9. Transmission electron micrographs (cross sectional view) of the ultrathin sections of the solvent-cast films of PAS-8 (A), PAS-14 (B), PAS-24 (C), PAS-41 (D), and PAS-71 (E). The black area is the PDMS domain stained with RuO_4, and the white area corresponds to the aramid domain.

for studying the morphology of microphase-separated structures in block and graft copolymers. It has recently been utilized for surface structure visualization. For example, the surface structures of polyisoprene-*b*-polystyrene,[12,13] polybutadiene-*b*-polystyrene,[13,34,35] poly(methyl methacrylate)-*b*-polystyrene,[36] poly(2,3-dihydroxypropyl methacrylate)-*b*-polystyrene,[19] poly(2-hydroxyethyl methacrylate)-*b*-polystyrene (poly(2-hydroxyethyl methacrylate) = PHEMA),[20] and PHEMA-*b*-polyisoprene[21] were observed under TEM.

Cross-sectional TEM views in the near-surface region of the PAS films that were cast from DMAc are shown in Figure 9. The upper part is an embedding epoxy resin which corresponds to the air side of the sample film. In these images, the black area indicates a PDMS domain that was stained with RuO_4, and the white area corresponds to an aramid domain. Room-temperature microtoming is very difficult for PAS films without staining of RuO_4 that contains greater than 41 wt % PDMS due to the flexibility of the films. Hence the films were exposed to RuO_4 vapor for 15 min in order to fix and stain the structure. It was very easy to obtain ultrathin sections from the fixed film with RuO_4. However, it is preferable to shorten the staining time because the RuO_4 vapor has a strong oxidation power. When a PAS film with 71 wt % PDMS was exposed to RuO_4 vapor for 30 min, the film surface was considerably destroyed. Staining for 15 min gave good results.

In order to confirm the absence of morphological change by means of various pretreatments (RuO_4 exposure, embedding in epoxy resin, and sectioning at room temperature), TEM observation of the cryotomed ultrathin section of PAS-71 was also performed. This ultrathin section was cut at −120 °C using an Ultracut E that was equipped with an FC4E cryosectioning attachment, Reichert-Jung, Vienna, Austria. PDMS's high electron density (as compared to aramid) contributes to sufficient contrast without staining. As a result, there was no morphological difference between the images obtained by general sectioning at room temperature and by cryosectioning.

In the bulk phase of PAS-8, PAS-14, and PAS-24, discrete spherical regions of PDMS in an aramid matrix are shown in parts A−C of Figure 9. The diameters of the spherical domains of PAS-8, -14, and -24 showed approximately the same values (100−150 Å). On the other hand, however, the distances between the PDMS spheres gradually decreased with increasing PDMS content. This result may be attributable to the molecular weight of the PDMS and aramid segments. Since all of the PASs contain the same molecular weight of PDMS (Table 1), the similar size micelles with PDMS cores may be generated in the DMAc solution and then form PDMS spheres during the casting process. Similarly, the distance between the PDMS spheres in an aramid matrix may be due to the degree of polymeri-

zation of the aramid components that control the in bulk composition of aramid and PDMS. Although a spherical microphase-separated structure was observed in bulk, the top surface was covered with a continuous PDMS layer (stained with RuO_4) in order to minimize surface energy. The top layers were approximately 10−20 and 50 Å thickness for PAS-8 and -14, and PAS-24, respectively. The presence of the PDMS layer at the top surface of the PAS-8, -14, and -24 films correspond to the results of angular-dependent XPS and SSIMS measurements.

In the bulk phase of PAS-41, cylinder (dispersed PDMS cylinders in an aramid matrix) or lamellar-like microphase-separated structures were observed as shown in Figure 9D, and the top surface was also completely covered with a PDMS layer (ca. 50 Å thickness). This was consistent with the results from angular-dependent XPS and SSIMS measurements. When PAS-41's bulk morphology is compared to that of PASs with a PDMS content of 8−24 wt %, there is a difference in the PDMS domain connecting state. In PAS-8, -14, and -24, the PDMS domains exist discretely in an aramid matrix. The PDMS domains in PAS-41, however, connect continuously although they do not form a matrix. In our previous study, we reported that PAS films with a PDMS content that was greater than 35 wt % showed excellent gas permeability, thereby suggesting the continuity of the PDMS phase.[26] We visually confirmed the bulk morphology of PAS films by TEM observation and elucidated the correlation between the gas permeability and the PDMS content in PAS.

A cross sectional TEM image of PAS-71 is shown in Figure 9E. Contrary to our expectations, the PDMS spherical microdomain structure was observed although the volume fraction of PDMS in PAS-71 was 0.8. It was calculated by using the group contributions to the molar volume.[37] This may be attributable to the effects of a casting solvent. Since DMAc is a selectively poor solvent for PDMS, the molecular chain of PDMS can not spread extensively in the DMAc solution and generates micelles. When the solution is concentrated to form a solid film in the casting process, the structure of the PDMS micelles may be maintained. Hence, similar to PAS-41 film morphology, the PDMS domains in the PAS-71 film also connected three dimensionally. This led to high gas permeability compared with conventional silicone rubber. Since both the molecular weight and the volume fraction of the aramid segments are very small (M_n = 700; volume fraction = 0.2), it may be impossible to form an aramid matrix in bulk even if DMAc is a selectively good solvent for aramid. This belief is supported by the absence of the T_g of aramid component in PAS-71 as obtained by dynamic thermomechanical analysis.[26]

The top surface of the PAS-71 film was also covered with continuous PDMS micelles (ca. 100 Å diameter). The size was approximately equal to that in bulk. This may be attributable to differences in solid film formation in the casting process. Since the PDMS micelles of PAS-71 in the DMAc solution are not completely covered with aramid segments due to its low volume fraction, the top surface of the PAS-71 film may be covered with PDMS micelles without restructuring of the microdomain. When PAS contains less than 41 wt % PDMS, the PDMS micelles can be wrapped with an aramid segment in the DMAc solution. Consequently the restructuring of the microdomain occurs, affording a PDMS layer in the top surface area to minimize the surface free energy.

In this study, the surface characterization of the aramid−poly(dimethylsiloxane) multiblock copolymers with 8, 14, 24, 41, and 71 wt % of PDMS was performed by angular-dependent XPS, static SIMS measurements, and TEM observation. All the analytical results show the surface enrichment of the lower surface energy PDMS segments in the outermost atomic layers. In particular, the top surfaces of all PAS films were completely covered with a thin PDMS layer although the microphase-separated structure in bulk was different according to the PDMS content in PAS. From these results, we can conclude that solvent-cast PAS films have variable mechanical properties ranging from a rubbery state to a glassy state with the same surface composition.

Acknowledgment. The authors would like to thank Ms. Toshie Oyama, Department of Composite Materials, National Institute of Materials and Chemical Research, for her assistance with XPS and SSIMS measurements. We could also like to thank Ms. Yoshiko Ito, Nissei Sangyo Co. Ltd., for sample preparation of cryotomed ultrathin sections. T.F. is indebted to the Japan Society for the Promotion of Science (JSPS Research Fellowships for Young Scientists) for research grants. This work was partly financially supported by a Grant-in-Aid for Scientific Research (No. 07558257) from the Ministry of Education, Science, and Culture, Japan, and a Grant-in-Aid for Research and Development Project of New Medical Technology in Artificial Organs from the Ministry of Health and Welfare, Government of Japan, in 1995 and Ciba-Geigy Foundation (Japan) for the Promotion of Science.

References and Notes

(1) For Part 1, see ref 21; for Part 2, see ref 22; for Part 3, see ref 23; for Part 4, see ref 24; for Part 5, see ref 25; for Part 6, see ref 26.
(2) Garbassi, F.; Morra, M.; Occhiello, E. In *Polymer Surfaces*; Garbassi, F., Morra, M., Occhiello, E., Eds; John Wiley & Sons: Chichester, England, 1994.
(3) Okano, T.; Nishiyama, S.; Shinohara, I.; Akaike, T.; Sakurai, Y.; Kataoka, K.; Tsuruta, T. *J. Biomed. Mater. Res.* **1981**, *15*, 393.
(4) Patel, N.; Dwight, D. W.; Hedrick, J. L.; Webster, D. C.; McGrath, J. E. *Macromolecules* **1988**, *21*, 2689.
(5) Smith, S. D.; DeSimone, J. M.; Huang, H.; York, G.; Dwight, D. W.; Wilkes, G. L.; McGrath, J. E. *Macromolecules* **1992**, *25*, 2575.
(6) Chen, X.; Gardella, J. A., Jr. *Polym. Prepr. (Am. Chem. Soc., Div. Polym. Chem.)* **1992**, *33* (2), 312.
(7) Chen, X.; Gardella, J. A., Jr.; Kumler, P. L. *Macromolecules* **1993**, *26*, 3778.
(8) Chen, X.; Lee, H. F.; Gardella, J. A., Jr. *Macromolecules* **1993**, *26*, 4601.
(9) Chen, X.; Gardella, J. A., Jr.; Kumler, P. L. *Macromolecules* **1992**, *25*, 6621, 6631.
(10) Tezuka, Y.; Nobe, S.; Shiomi, T. *Macromolecules* **1995**, *28*, 8251.
(11) Tezuka, Y.; Ono, T.; Imai, K. *J. Colloid Interface Sci.* **1990**, *136*, 408.
(12) Hasegawa, H.; Hashimoto, T. *Macromolecules* **1985**, *18*, 589.
(13) Hasegawa, H.; Hashimoto, T. *Polymer* **1992**, *33*, 475.
(14) Coulon, G.; Russell, T. P.; Deline, V. R.; Jerome, R. *Macromolecules* **1989**, *22*, 2581.
(15) Kajiyama, T.; Teraya, T.; Takahara, A. *Polym. Bull.* **1990**, *9*, 315.
(16) Yasuda, H.; Charlson, E. J.; Charlson, E. M.; Yasuda, T.; Miyama, M.; Okuno, T. *Langmuir* **1991**, *7*, 2394.
(17) Lewis, K. B.; Ratner, B. D. *J. Colloid Interface Sci.* **1993**, *159*, 77.
(18) Tezuka, Y.; Araki, A. *Langmuir* **1994**, *10*, 1865.
(19) Mori, H.; Hirao, A.; Nakahama, S.; Senshu, K. *Macromolecules* **1994**, *27*, 4093.
(20) Senshu, K.; Yamashita, S.; Ito, M.; Hirao, A.; Nakahama, S. *Langmuir* **1995**, *11*, 2293.
(21) Senshu, K.; Yamashita, S.; Mori, H.; Ito, M.; Hirao, A.; Nakahama, S. *Macromolecules*, submitted for publication.
(22) Kajiyama, M.; Kakimoto, M.; Imai, Y. *Macromolecules* **1989**, *22*, 4143.

(23) Furuzono, T.; Yashima, E.; Kishida, A.; Maruyama, I.; Matsumoto, T.; Akashi, M. *J. Biomater. Sci. Polym. Ed.* **1993**, *5*, 89.
(24) Kishida, A.; Furuzono, T.; Ohshige, T.; Maruyama, I.; Matsumoto, T.; Itoh, H.; Murakami, M.; Akash, M. *Angew. Makromol. Chem.* **1994**, *220*, 89.
(25) Furuzono, T.; Seki, K.; Kishida, A.; Ohshige, T.; Waki, K.; Maruyama, I.; Akashi, M. *J. Appl. Polym. Sci.* **1996**, *59*, 1059.
(26) Matsumoto, T.; Koinuma, Y.; Waki, K.; Kishida, A.; Furuzono, T.; Maruyama, I.; Akashi, M. *J. Appl. Polym. Sci.* **1996**, *59*, 1067.
(27) Furuzono, T.; Kishida, A.; Yanagi, M.; Matsumoto, T.; Kanda, T.; Nakamura, T.; Aiko, T.; Maruyama, I.; Akashi, M. *J. Biomater. Sci. Polym. Ed.* **1996**, *7*, 871.
(28) Furuzono, T.; Senshu, K.; Kishida, A.; Matsumoto, T.; Akashi, M. *Polym. J.* **1997**, *29*, 201.
(29) Lukas, J.; Jezek, B. *Collect. Czech. Chem. Commum.* **1983**, *48*, 2909.
(30) Briggs, D. In *Ion and Neutral Spectroscopy*; Briggs, D., Seah, M. P., Eds.; Practical Surface Analysis; Wiley: Chichester, 1992; Vol. 2.
(31) Trent, J. S.; Schenbeim, J. I.; Couchman, P. R. *Macromolecules* **1983**, *16*, 589.
(32) Trent, J. S. *Macromolecules* **1984**, *17*, 2930.
(33) Newman, J. G.; Carlson, B. A.; Michael, R. S.; Moulder, J. F.; Hohlt, T. A. In *Static SIMS Handbook of Polymer Analysis*; Newman, J. G., Carlson, B. A., Michael, R. S., Moulder, J. F., Hohlt, T. A., Eds.; Perkin-Elmer Corp., Physical Electronics Div.; Eden: Parie, MN, 1991.
(34) Annis, B. K.; Schwark, D. W.; Reffner, J. R.; Thomas, E. L.; Wunderlich, B. *Makromol. Chem.* **1992**, *193*, 2589.
(35) Schwark, D. W.; Vizie, D. L.; Reffner, J. R.; Thomas, E. L.; Annis, B. K. *J. Mater. Sci. Lett.* **1992**, *11*, 352.
(36) Russell, T. P.; Mayes, A. M.; Kunz, M. S. In *Ordering in Macromolecules Systems*; Teramoto, A., Kobayashi, M., Norisuye, T., Eds.; Springer-Verlag: Berlin, 1993; p 217.
(37) Fedors, R. F. *Polym. Eng. Sci.* **1974**, *14*, 147.

MA9616219